

Electromigration Model for Platinum Hotplates

Lado Filipovic

Institute for Microelectronics, Technische Universität Wien, 1040 Vienna, Austria
Email: filiptovic@iue.tuwien.ac.at, ORCID: 0000-0003-1687-5058

Abstract—Microheaters are frequently applied in the design of semiconductor metal oxide gas sensors in order to heat the sensing layer and induce the surface chemical reactions which promote molecular adsorption. One of the most common materials used for the microheater layer is platinum. In this manuscript, a model for electro-migration is developed and implemented to study vacancy dynamics and the thereby-induced stress in platinum-based microheaters for gas sensor applications. The model is then applied to study the impact of the individual components which contribute to vacancy transport, including electro-migration, thermo-migration, and stress-migration. We find that these structures have very high thermal gradients, making the impact of thermo-migration component higher than the electro-migration component in the early stages of vacancy transport, unlike in copper-based interconnects. Therefore, improving the temperature uniformity of the microheater design should lead to a longer operating time before failure.

Index Terms—Electromigration, platinum, microheater, Semiconductor metal oxide gas sensor

I. INTRODUCTION

There is a plethora of different types of sensors which are based on micro-electro-mechanical systems (MEMS) microheater technology and rely on an elevated temperature in order to enable the sensor's primary functionality. These high temperatures are commonly provided by an integrated micro-heater or hotplate. Typical examples of such sensors are chemoresistive gas sensors based on semiconductor metal oxide (SMO) films [1] and nondispersive infrared (NDIR) optical gas sensors [2]. In SMO sensors, the MEMS heater is applied to elevate the sensing film's temperature to values between 200°C and 500°C in order to enable the surface chemical reaction to take place, while NDIR optical gas sensors require temperatures above 500°C to provide the infrared emission source [2]. A typical schematic of the layers composing the membrane of the hotplate is given in Figure 1(a). Here, we note the presence of a heat spreading plate, which is not electrically connected, but serves to help reduce the temperature gradient in the sensing layer [3]. A typical top view of the structure is shown in Figure 1(b), where we note the suspension beams, which hold the heated components above the silicon wafer, creating the air cavity. At the required high temperatures and current densities, electromigration (EM) may lead to a failure in the hotplate's metallization lines [4], [5]. More importantly, the inherent non-uniformity in the temperature distribution may exacerbate the thermo-migration (TM) effect, as the migration of vacancies increases with increasing temperature gradients [6].

In order to satisfy the industry's push towards More-than-Moore integration [7] and reduce the cost of sensor fabrica-

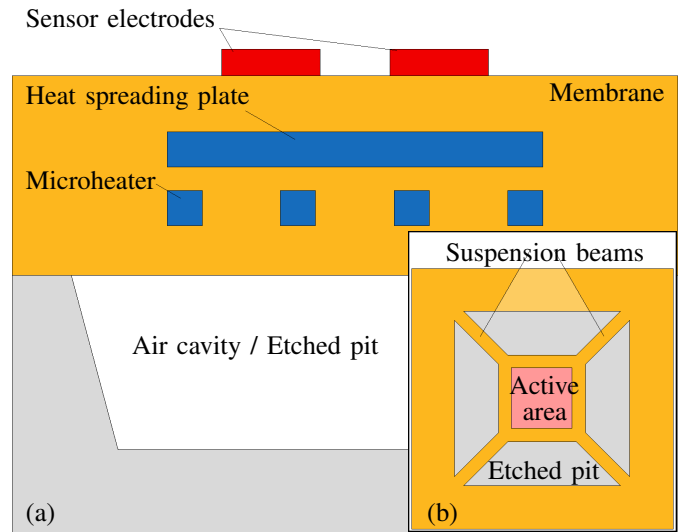


Fig. 1. (a) Two-dimensional cross-cut schematic of the layers composing the membrane of the hotplate and (b) the top view of the suspended membrane used in SMO gas sensors, showing the suspension beams, used to suspend the heated components in air above the silicon wafer.

tion, the entire sensor, including the microheater element and membrane which houses it, should be fabricated using complementary metal oxide semiconductor (CMOS) technology, which means that the heater material should be available in a CMOS fabrication facility. While initially polysilicon and aluminum were used, these materials were quickly shown to be prone to oxidation and early EM failure. Therefore, the most common materials used in CMOS-integrated hotplates today are platinum [1] and tungsten [8]. Tungsten, while being practically EM resistant, tends to form an oxide when exposed to air at high temperatures [9]. Platinum, on the other hand, is very stable, has a linear temperature response, and is resistant to oxidation at a broad range of operating temperatures [1]. Nevertheless, there is some evidence of degrading EM behavior in thin platinum lines [5], which is very difficult to quantify experimentally since there are always more effects influencing the different material stacks at very high operating temperatures, including diffusion of atoms from the adhesion layer, thermal expansion, and cracking and delamination [10]. Using published material parameters for atom and vacancy diffusivity in platinum, we have devised an EM model for microheater applications. Using this model, we are able to study the impact of EM, including thermo-migration and stress-migration, on microheaters and micro-

heater arrays for SMO sensor applications. Furthermore, we quantify the importance temperature uniformity on the EM reliability. Previously, we have already shown that improving the uniformity results in a faster return to the sensor baseline and improved sensitivity [11].

II. ELECTROMIGRATION MODEL

A physical description of EM is provided in [12], where the driving force for EM failure is shown to stem from the accumulation of vacancies, leading to increased tensile stress and the generation of a void which can cause immediate cracking or it can grow under further EM stress to induce open-circuit failure. At the same time, the reduction of vacancies, or accumulation of atoms, at the other end of the metal line forms hillocks, resulting in a compressive stress. To model the EM phenomena, three components must be solved at each simulation time step, as shown by Algorithm 1 in Figure 2: The electro-thermal problem, vacancy dynamics, and solid mechanics. The electro-thermal problem determines the electric field and induced temperature gradient in the structure, the vacancy dynamics problem calculates the movement of vacancies through the line, and the solid mechanics components calculates the stress and strain induced by the accumulation of vacancies. Usually, EM simulations are performed under accelerated conditions, achieved by applying a very high current density and high ambient temperature. Thereafter, using Black's equation, the behavior can be extrapolated back to operating conditions in order to find the time to failure under normal operating conditions [5], [13], [14].

To simulate EM in microheaters, only an increased current density is applied and the ambient temperature is kept at room temperature. The high current density and electric field in the platinum layer create a high temperature by Joule heating. Not prescribing a static temperature allows to form natural temperature gradients in the simulated microheater, which is commonly ignored when performing EM simulations in, e.g., copper interconnects [13], [15], but is essential in metal lines which potentially have a non-uniform temperature distribution. Since EM simulations are typically very time consuming, even for simple interconnect lines, in order to enable EM modeling for complex micro-hotplate geometries and membranes, we propose an accelerated approach. For this approach, first the steady state solution to the electro-thermal problem is found and the result is used when solving vacancy dynamics and solid mechanics in the time dependent simulation, depicted by Algorithm 2 in Figure 2. This is appropriate in the case of EM modeling since the final current density and temperature distribution in the platinum film is usually reached in under one ms [3], while EM phenomena is observed at times many orders of magnitude higher [5].

The electro-thermal problem solves the heat equation to find the temperature induced by the applied current; then the vacancy migration dynamics is solved to find the vacancy concentration inside the platinum layer; finally, the mechanical problem is solved to find the stress induced due to the accumulation of vacancies [13]. Calculating the vacancy dynamics

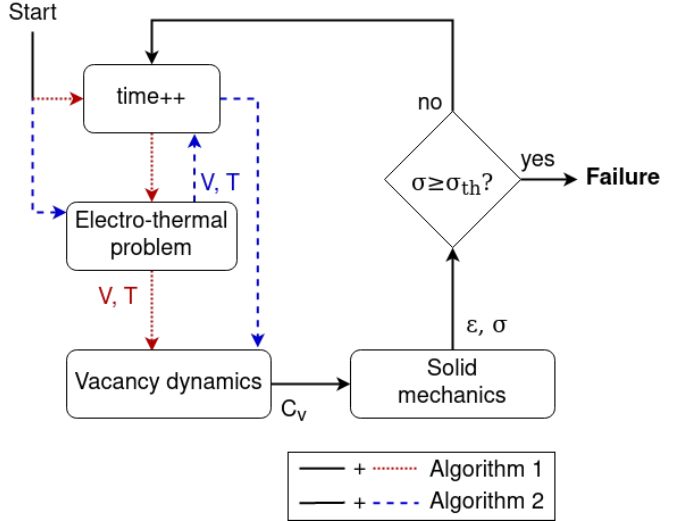


Fig. 2. Flowchart for the electro-migration model showing the paths for Algorithm 1 (dotted red): The electro-thermal problem is solved at every time step and Algorithm 2 (dashed blue): Steady-state solution for the electro-thermal problem is found prior to time discretization. The black arrows apply to both algorithms

is at the core of EM modeling. The change in the vacancy concentration C_v in time t is found by summing the effects of the vacancy flux \vec{J}_v and vacancy generation/annihilation G . The equation which governs this mechanism is given by

$$\frac{\delta C_v}{\delta t} = -\nabla \cdot \vec{J}_v + G, \quad (1)$$

where the vacancy flux is determined by the diffusivity D_v and the sum of the individual EM, TM, and stress-migration (SM) components, represented by $eZ^*\nabla\varphi$, $Q^*\nabla T/T$, and $f\Omega\nabla\sigma$, respectively, by

$$\vec{J}_v = -D_v \left[\nabla C_v + \frac{C_v}{kT} \left(eZ^*\nabla\varphi - \frac{Q^*}{T}\nabla T + f\Omega\nabla\sigma \right) \right], \quad (2)$$

where k is the Boltzmann constant, T is temperature, e is the elementary charge, φ is the electrical potential, and σ is the induced stress. The other parameters used in the model and their values in the case of platinum are given in Table I. The vacancy diffusivity also depends on the induced stress and is calculated using

$$D_v = D_{v0} \exp \left(\frac{\Omega\sigma - E_a}{kT} \right). \quad (3)$$

The vacancy generation/annihilation term G from Eq. (1) is calculated using the Rosenberg-Ohring function [16]

$$G = \frac{1}{\tau} (C_v - C_{v0}), \quad (4)$$

which is applied at the grain boundaries and material interfaces. When an atom is exchanged by a vacancy, the effective volume change leads to the build-up of strain [17], and ultimately in a stress σ . The stress is determined by Hooke's law, assuming elastic material properties [18]. Once

the induced stress reaches a critical threshold σ_{th} , the metal layer will either crack or a void will form, which then grows, increasing the line resistance, until an effective open circuit failure is induced.

TABLE I
PUBLISHED PARAMETERS WHICH WERE USED FOR THE EM SIMULATION OF PLATINUM MICROHEATERS.

Sym.	Description	Value	Ref.
C_{v0}	Equilibrium vacancy concentration	$1.07 \times 10^{16} \text{ cm}^{-3}$	[19]
D_{v0}	Pre-exponential factor for vacancy diffusivity	$0.22 \text{ cm}^2 \text{ s}^{-1}$	[20]
E_a	Activation energy for diffusion	2.89 eV	[20]
f	Vacancy relaxation factor	0.5	[21]
Ω	Atomic volume of Pt	$1.51 \times 10^{-29} \text{ m}^3$	-
Q^*	Heat of transport	0.68 eV	[6]
τ	Vacancy relaxation time	200ms	[22]
Z^*	Effective valence	0.3	[23]

III. RESULTS AND DISCUSSION

To assess the reliability of the microheater, only the membrane is simulated, while the silicon wafer below is ignored, as it does not contribute to the EM phenomena. The membrane is suspended using four arms, which are attached to the silicon wafer and are used as fixed points for the mechanical simulation, as shown in Figure 1. The presented model is applied to study EM in a typical meander microheater on a $1.8\mu\text{m} \times 1.8\mu\text{m}$ membrane with platinum lines with a cross section of $100\text{nm} \times 100\text{nm}$ and a 200nm pitch, embedded in a 300nm thick SiO_2 membrane, shown in Figure 3. A current density of 11.3MA/cm^2 , corresponding to a power dissipation of 0.77mW , was applied in order to reach a temperature of 1660°C at the center of the membrane, which drops to about 1600°C at the membrane edges. Heat conduction through the suspension beams and air, as well as air convection were applied in order to obtain a realistic temperature profile for the applied power.

After performing the time-dependent EM simulation on this structure for a period of 10^6 seconds, with the top and bottom of the membrane exposed to air, the resulting maximum EM-induced stress is calculated, as shown in Figure 4. We note that Algorithm 2 provides no loss of accuracy while reducing the simulation time by 40% compared to Algorithm 1. Furthermore, the obtained stress is near 1GN/m^2 , which is significant enough to suggest that it needs to be considered when designing microheaters. Currently, most studies only look at the intrinsic and thermal stresses when evaluating the mechanical stability of the proposed designs, while EM is largely ignored [10].

The implementation of this model also allows to analyze the individual contributions to vacancy dynamics which can be from EM ($eZ^*\nabla\varphi$), TM ($Q^*\nabla T/T$), and SM ($f\Omega\nabla\sigma$) components from Eq. (2). These are shown in Figure 5, where it is clear that, as expected, SM becomes the main driving force in the later stages. It is noteworthy that the temperature non-uniformity, which results in an increased

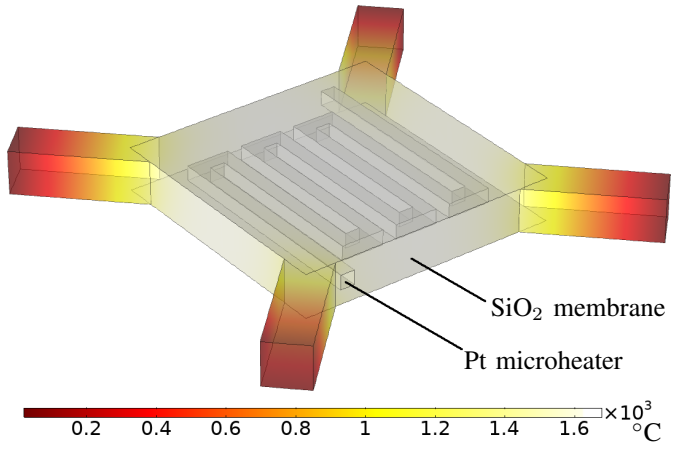


Fig. 3. Temperature ($^\circ\text{C}$) and geometry of a typical meander platinum hotplate in an SiO_2 membrane after applying a current density of 11.3MA/cm^2 , reaching a maximum temperature of 1600°C . The pitch of the microheater lines is 200nm with a cross-section of $100\text{nm} \times 100\text{nm}$.

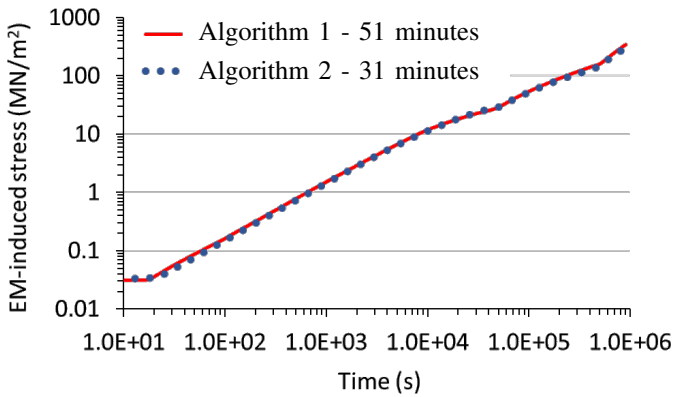


Fig. 4. EM-induced stress when applying 11.3MA/cm^2 to the microheater from Figure 3 using Algorithm 1 and Algorithm 2 from Figure 2.

temperature gradient and thereby in TM, has a significant impact in the early stages of vacancy transport. In fact, for this hotplate design, the ∇T component has a slightly greater impact than the $\nabla\varphi$ component, which is not the case for copper (Cu) interconnects. The differences in the impact of EM and TM components in the meander hotplate is visually shown in Figure 6. When we analyze the individual terms in previous Cu studies [13], it can be observed that the $\nabla\varphi$ component is three orders of magnitude larger than the ∇T component. From this, we can conclude that the vacancy-induced reliability for platinum-based hotplates is significantly impacted by temperature gradients in the metal lines and that the lifetime of these devices can be improved by improving the temperature uniformity.

IV. CONCLUSION

A model for vacancy dynamics under the influence of EM and TM in platinum micro-hotplates is presented, along with two algorithms for its solution. The first algorithm solves all required steps, which includes the electro-thermal, the vacancy

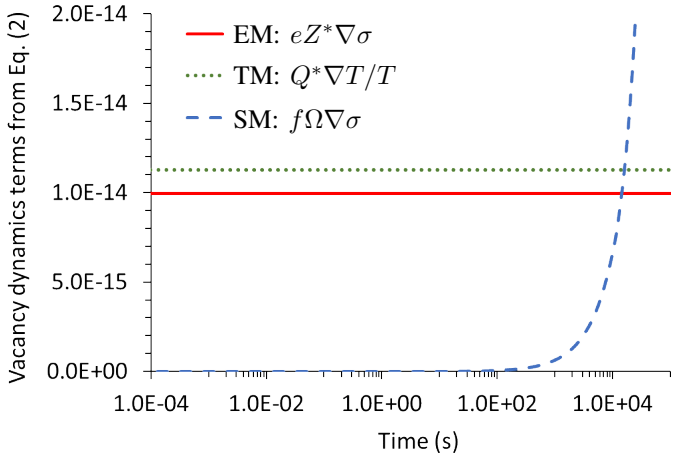


Fig. 5. Maximum contributions from different components from Eq. (2) to the vacancy dynamics in platinum microheaters. It is evident that the temperature non-uniformity (∇T) plays a significant role in EM.

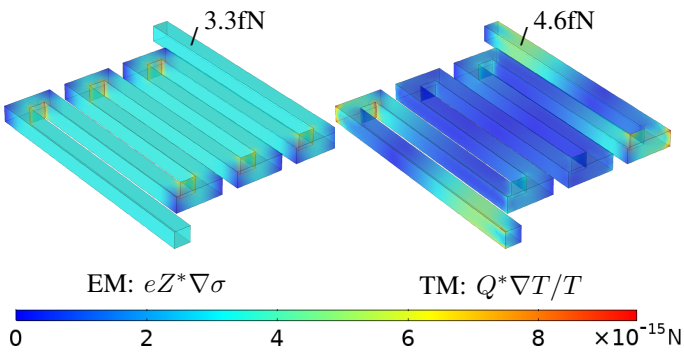


Fig. 6. Distribution of the EM and TM components of the vacancy dynamics model in a typical platinum meander microheater, shown in Figure 3.

dynamics, and the mechanical stress components, at every time step, while the second accelerated algorithm calculates the static electro-thermal component once and then applies this solution to the time-discretized vacancy dynamics calculation. This ultimately allowed for a 40% speedup in the simulation of a platinum-based meander microheater with no loss in accuracy. This is possible due to the fact that the potential and temperature distribution in the microheater reach a steady-state in less than one millisecond, while EM requires a much larger time-scale. The accelerated algorithm was then applied to study the impact of temperature non-uniformity on the lifetime of the aforementioned microheater. We found that the thermal component is larger than the electrical component in these devices, meaning that high temperature gradients in such microheaters could induce premature failure.

REFERENCES

- [1] A. Lahllalia, L. Filipovic, and S. Selberherr, "Modeling and simulation of novel semiconducting metal oxide gas sensors for wearable devices," *IEEE Sensors Journal*, vol. 18, no. 5, pp. 1960–1970, 2018, doi: [10.1109/JSEN.2018.2790001](https://doi.org/10.1109/JSEN.2018.2790001).
- [2] D. Popa and F. Udrea, "Towards integrated mid-infrared gas sensors," *Sensors*, vol. 19, no. 9, pp. 2076(1–15), 2019, doi: [10.3390/s19092076](https://doi.org/10.3390/s19092076).
- [3] L. Filipovic and S. Selberherr, "Thermo-electro-mechanical simulation of semiconductor metal oxide gas sensors," *Materials*, vol. 12, no. 15, pp. 2410–1–2410–37, 2019, doi: [10.3390/ma12152410](https://doi.org/10.3390/ma12152410).
- [4] J. Spannhake, A. Helwig, G. Müller, G. Faglia, G. Sberveglieri, T. Doll, T. Wassner, and M. Eickhoff, "SnO₂:Sb – A new material for high-temperature MEMS heater applications: Performance and limitations," *Sensors and Actuators B: Chemical*, vol. 124, no. 2, pp. 421–428, 2007, doi: [10.1016/j.snb.2007.01.004](https://doi.org/10.1016/j.snb.2007.01.004).
- [5] R. Rusanov, H. Rank, T. Fuchs, R. Mueller-Fiedler, and O. Kraft, "Reliability characterization of a soot particle sensor in terms of stress- and electromigration in thin-film platinum," *Microsystem Technologies*, vol. 22, no. 3, pp. 481–493, 2015, doi: [10.1007/s00542-015-2576-6](https://doi.org/10.1007/s00542-015-2576-6).
- [6] S. Ho, T. Hehenkamp, and H. Huntington, "Thermal diffusion in platinum," *Journal of Physics and Chemistry of Solids*, vol. 26, no. 2, pp. 251–258, 1965, doi: [10.1016/0022-3697\(65\)90152-6](https://doi.org/10.1016/0022-3697(65)90152-6).
- [7] W. Arden, M. Brillouët, P. Cogez, M. Graef, B. Huizing, and R. Mahnkopf, "More-than-Moore white paper," 2010, online: http://itrs2.net/uploads/4/9/7/7/49775221/irc-itrs-mtm-v2_3.pdf.
- [8] S. Z. Ali, A. D. Luca, R. Hopper, S. Boual, J. Gardner, and F. Udrea, "A low-power, low-cost infra-red emitter in CMOS technology," *IEEE Sensors Journal*, vol. 15, no. 12, pp. 6775–6782, 2015, doi: [10.1109/jsen.2015.2464693](https://doi.org/10.1109/jsen.2015.2464693).
- [9] A. Warren, A. Nylund, and I. Olefjord, "Oxidation of tungsten and tungsten carbide in dry and humid atmospheres," *International Journal of Refractory Metals and Hard Materials*, vol. 14, no. 5-6, pp. 345–353, 1996, doi: [10.1016/s0263-4368\(96\)00027-3](https://doi.org/10.1016/s0263-4368(96)00027-3).
- [10] R. Coppeta, A. Lahllalia, D. Kozic, R. Hammer, J. Riedler, G. Toschkoff, A. Singulani, Z. Ali, M. Sagmeister, S. Carniello, S. Selberherr, and L. Filipovic, "Electro-thermal-mechanical modeling of gas sensor hotplates," in *Sensor Systems Simulations*. Springer International Publishing, 2019, pp. 17–72, doi: [10.1007/978-3-030-16577-2_2](https://doi.org/10.1007/978-3-030-16577-2_2).
- [11] A. Lahllalia, O. L. Neel, R. Shankar, S. Selberherr, and L. Filipovic, "Improved sensing capability of integrated semiconducting metal oxide gas sensor devices," *Sensors*, vol. 19, no. 2, pp. 374(1–14), 2019, doi: [10.3390/s19020374](https://doi.org/10.3390/s19020374).
- [12] H. Ceric, H. Zahedmanesh, and K. Croes, "Analysis of electromigration failure of nano-interconnects through a combination of modeling and experimental methods," *Microelectronics Reliability*, vol. 100–101, pp. 113 362(1–6), 2019, doi: [10.1016/j.microrel.2019.06.054](https://doi.org/10.1016/j.microrel.2019.06.054).
- [13] L. Filipovic, "A method for simulating the influence of grain boundaries and material interfaces on electromigration," *Microelectronics Reliability*, vol. 97, pp. 38–52, 2019, doi: [10.1016/j.microrel.2019.04.005](https://doi.org/10.1016/j.microrel.2019.04.005).
- [14] J. Black, "Electromigration failure modes in aluminum metallization for semiconductor devices," *Proceedings of the IEEE*, vol. 57, no. 9, pp. 1587–1594, 1969, doi: [10.1109/proc.1969.7340](https://doi.org/10.1109/proc.1969.7340).
- [15] R. de Orio, H. Ceric, and S. Selberherr, "Physically based models of electromigration: From Black's equation to modern TCAD models," *Microelectronics Reliability*, vol. 50, no. 6, pp. 775–789, 2010, doi: [10.1016/j.microrel.2010.01.007](https://doi.org/10.1016/j.microrel.2010.01.007).
- [16] R. Rosenberg and M. Ohring, "Void formation and growth during electromigration in thin films," *Journal of Applied Physics*, vol. 42, no. 13, pp. 5671–5679, 1971, doi: [10.1063/1.1659998](https://doi.org/10.1063/1.1659998).
- [17] H. Ceric, R. Heinzl, C. Hollauer, T. Grasser, and S. Selberherr, "Microstructure and stress aspects of electromigration modeling," in *AIP Conference Proceedings*, vol. 817, 2006, pp. 262–269, doi: [10.1063/1.2173558](https://doi.org/10.1063/1.2173558).
- [18] R. Kirchheim, "Stress and electromigration in Al-lines of integrated circuits," *Acta Metallurgica et Materialia*, vol. 40, no. 2, pp. 309–323, 1992, doi: [10.1016/0956-7151\(92\)90305-x](https://doi.org/10.1016/0956-7151(92)90305-x).
- [19] A. Seville, "Effects of vacancies on the physical properties of platinum," *Platinum Metals Review*, vol. 19, no. 3, pp. 96–99, 1975, online: <https://www.technology.matthey.com/pdf/pmr-v19-i3-096-099.pdf>.
- [20] F. Cattaneo, E. Germagnoli, and F. Grasso, "Self-diffusion in platinum," *Philosophical Magazine*, vol. 7, no. 80, pp. 1373–1383, 1962, doi: [10.1080/14786436208213170](https://doi.org/10.1080/14786436208213170).
- [21] A. Čížek and V. Doláková, "A dilatometric study of platinum during repeated quenching," *Czechoslovak Journal of Physics*, vol. 22, no. 4, pp. 302–310, 1972, doi: [10.1007/bf01689616](https://doi.org/10.1007/bf01689616).
- [22] A. H. Seville, "Studies of the specific heat of platinum by modulation methods," *Physica Status Solidi (a)*, vol. 21, no. 2, pp. 649–658, 1974, doi: [10.1002/pssa.2210210230](https://doi.org/10.1002/pssa.2210210230).
- [23] J. P. Dekker, A. Lodder, and J. van Ek, "Theory for the electromigration wind force in dilute alloys," *Physical Review B*, vol. 56, no. 19, pp. 12 167–12 177, 1997, doi: [10.1103/physrevb.56.12167](https://doi.org/10.1103/physrevb.56.12167).